International Journal of Science and Research (IJSR)
ISSN: 2319-7064
SJIF (2022): 7.942

Hydrogenation of Palm Esters to Fatty Alcohols using $Re/Nb/Al_2O_3$ Catalysts

Germildo J. Muchave[1*], João M. A. R. Almeida[2], Donato A. G. Aranda[1]

[1]EPQB, Escola de Química, Universidade Federal do Rio de Janeiro, Av. Athos da Silveira Ramos, 149, RJ, 21941-909, Brazil
[2]Instituto de Química/ Universidade Federal do Rio de Janeiro, Av. Athos da Silveira Ramos, 149, RJ, 21044-020, Brazil

[*]Corresponding Author, E-mail: germildomuchave [at]gmail.com

Abstract: ***The catalytic hydrogenation of palm esters to obtain fatty alcohols using Re-x%Nb/Al_2O_3 catalysts was evaluated without solvents. The catalysts were characterized using nitrogen physisorption, X-ray Diffraction, X-ray Photoelectron Spectroscopy, Temperature-Programmed-Reduction, Pyridine-FTIR, and Temperature-Programmed-Desorption-NH_3. The catalyst with a 10% Nb load was the one that obtained better performance when compared to the other catalysts with 5Nb and 20%Nb. The catalyst with 10%Nb obtained an average of 90% ester conversion and 79% selectivity in fatty alcohols. The design of experiments was made to understand the most important variable in the system. The results showed that temperature and pressure were the most critical factors. The better catalytic performance obtained employing the 10% Nb catalyst can be explained by its acidity properties. Moreover, this catalyst showed high stability in the deactivation assays. The results obtained in this work showed a promising method to obtain catalysts with high performance to produce fatty alcohols. Thermodynamic reasons (temperature and pressure) justify the slow conversion rate of wax esters to fatty alcohols for most reactions.***

Keywords: Catalysis, Palm Esters, Fatty Alcohols

1.Introduction

Catalytic hydrogenation has contributed to the growth of the oleochemical industry. This process has been applied to obtain several high valued products, such as hydrocarbons (aviation kerosene, green diesel, and biogasoline) [1]; wax esters [2]; fatty alcohols [3, 4]. Fatty alcohols, for example, are very important in the industry as they are intermediates for several products; for example, fatty alcohols are used in the manufacture of nonionic surfactants, cosmetics, shampoos, conditioners, resins, food supplements, lubricants, and the production of green hydrocarbons. About 50% of the volume of fatty alcohols produced annually is destined mainly for synthesizing anionic and ionic surfactants [5]. However, the production of fatty alcohols remains a challenge due to the high cost of catalysts, and the current chromium-basedcatalysts have environmental implications [6–8].

Recently, attempts have been made to develop new catalysts to produce fatty alcohol under mild conditions to replace classic catalysts (Cu-Cr) [3, 9, 10]. The Cu-Cr catalyst is effective in terms of catalytic and selective activity; nevertheless, it is not environmentally safe because of the presence of chromium in its composition. Besides that, the conventional method of fatty alcohol production applies Cu-Cr catalyst in severe conditions between 250-300^{o}C of temperature and 2000-3000 Psi of H_2 pressure [11].

The application of noble metal catalysts for obtaining fatty alcohols by hydrogenation has been most important in the last years. Some noble metal-based catalysts were used, with emphasis of ruthenium [12, 13], platinum [14], palladium [15, 16]; and rhenium [3]. Nevertheless, despite being efficient in hydrogenation reactions, it is necessary to control the process conditions to avoid the formation of unwanted products (hydrocarbons, for instance). Other catalysts systems without noble metals but with other metals such as Cu-Mn [17], Cu-Fe [18], and Cu-Zn [19] have also been developed.

Rhenium is one of the few metals highly active in its activity for partial removal of oxygen from oils and their derivatives, producing alcohol in the corresponding carbon chain [3, 4, 20]. [21] considers that the effectiveness of the monometallic rhenium catalyst for the production of fatty alcohols can be improved with the addition of promoters, mainly of noble metals (ruthenium, rhodium, platinum, and palladium). Niobium is mainly used as a co-catalyst as a replacement for noble metals. For example, [22–24] have shown that the niobium has excellent potential in numerous catalytic applications, both as a promoter and support. For examples of niobium applications that have stood out are selective oxidation processes, hydrocarbon conversion, polymerization, elimination of pollutants (NOx), dehydrogenation, hydrotreatment, and electrochemistry [24].

No studies in the literature used niobium as a co-catalyst in the hydrogenolysis of fatty acids or esters to obtain fatty alcohols. In this work, the influence of niobium content as a promoter in bimetallic catalysts (Re-x%Nb/Al_2O_3) is studied for fatty alcohols production. Moreover, the preparation of rhenium-based catalyst was also evaluated.

2.Materials and Methods

2.1. Reagents

The following reagents were used to carry out the work: palm oil methyl ester [(Agropalma SA), the composition of palm biodiesel was: methyl palmitate (43.5%), linoleate

(10.2%), methyl oleate (39.8%) and methyl stearate (4.3%)], Perrenic Acid ($HReO_4$, Sigma-Aldrich), Niobium ammonium oxalate { (NH_4 [NbO (C_2O_4)$_2$ (H_2O)$_2$]. (H_2O) n, CBMM}, deionized water (H_2O), Hydrogen 99.99% (Linde Gases), alumina (γ-Al_2O_3, SASOL).

2.2. Catalyst Synthesis

The catalysts were prepared using two techniques: wet impregnation of niobium ammonium oxalate in alumina to form mixed support (x%Nb-Al_2O_3). Then, Rhenium (Re_2O_7) from the perrenic acid solution was incorporated through impregnation on x%Nb-Al_2O_3.In wet impregnation; the niobium ammonium oxalate was weighed and dissolved in deionized water with a specific amount of niobium. Then, the dissolved solution was placed in a 500 ml volumetric flask and added alumina to the same flask. The flask was placed in the rotavaporator under the agitation of 80 rpm for 2 hours. After this period, the rotavaporator was turned on at 80^{o}C under vacuum with continuous agitation to dry the samples. After synthesizing the double supports, they were placed in the oven for 12 hours at 100^{o}C. After 12h, the material (x%Nb/Al_2O_3) was removed from the oven and calcined at 200^{o}C for 2 hours. Finally, the rhenium was impregnated in the previously calcined material through the incipient wetness method. After impregnating rhenium in all substrates, they were calcined at 500^{o}C for 4 hours, with a heating rate of 5°C/min. The rhenium content in all catalysts was 4% (wt/wt).

2.3. Characterization of catalysts

The X-ray diffraction analysis was carried out on a Rigaku Miniflex II diffractometer with CuKα radiation (30 kV and 15 mA). The measurements was used under an angular scan ranging from 5º to 90º, increment of 0.05, and counting time of 1s/step without a knife.

Using the Micromeritics A.S.A.P. 2020, the surface area, volume, and pore size of the prepared catalysts were determined. First, 0.3g mass samples were taken in each catalyst. The samples were pretreated at 300^{o}C for 12 hours under constant vacuum in the same equipment and then analyzed. The specific surface area was obtained using the BET method and pore volume by the BJH method.

The TPR characterization of the catalysts was performed in the Micromeritics Autochem TPR-2920 Crycooler II equipment. We first weighed 30 mg of the catalyst samples, and then the samples were inserted into a quartz reactor with a heating ramp and temperature control. The samples were pretreated by an argon current at a 40 mL/min rate at 120^{o}C for 1h to reduce humidity. The analysis was performed under standard mixing flow of H_2 and Ar (10% H_2/Ar) at a 50 mL/min flow rate, with a heating ramp of 25^{o}C to 1000^{o}C and a heating rate of 10^{o}C/min.

The analyses were performed using a Thermo Scientific Escalab 250Xi spectrometer. The pressure inside the vacuum chamber was kept below 5 x 10^{-9} mbar. An Al Kα X-ray monochromatized radiation (hν = 1486.6 eV) was used as an X-ray source and operated at 216 W. The pass energy of the spectrometer was 100 eV and 25 eV for the XPS survey and core-level spectra, respectively. C1s (284.8 eV) were used for binding energy calibration. The data acquisition and peak fitting were performed using Thermo Avantage© software.The analyzes of the ammonia were carried out in a mass spectrometer QMS-200 (Balzers), with the ratio m/z=15, used to quantify the ammonia.

Ammonia adsorption was carried out at a temperature of 70°C using a 4% NH_3/He mixture with a flow rate of 30 mL.min-1 for 30 minutes; after this period, a purge with pure He was performed for 60 minutes. The desorption of the chemisorbed ammonia was carried out by heating the samples to 800°C at a rate of 20°C.min^{-1}. The desorbed ammonia was quantified from the catalysts by integrating the area under the intensity versus the time curve.

The Fourier transform infrared spectroscopy (FTIR) of pyridine was applied to determine the catalysts' Lewis and Bronsted acid sites. For this, the Shimadzu IRPrestige-21 equipment was used. About 0.1g of catalyst was weighed into a flask. Then, 1 ml of pyridine in the liquid phase was added and stirred manually. Then, the flask was placed in an oven at 100°C for pyridine evaporation. After drying, the sample was analyzed with FTIR, in the range of 1400-1580 cm-1, with a resolution of 2 cm^{-1} and a scan.

2.4. Catalytic Hydrogenation Tests

The experiments were carried out in a Parr Instruments batchreactor of 300 mL volume, with stainless steel cup, automatic temperature, and pressure control. The catalysts were pre-reduced in an oven with H_2 flux at 400^{o}C for 4 hours at a heating rate of 5^{o}C/min. Then, they were placed in the reactor cup and fed to the substrate. Finally, the reactor was pressurized with hydrogen to remove the air.4% (wt/wt) of the catalyst was placed on palm methyl ester for each reaction. The reactions proceeded with a stirring speed of 1200 rpm to reduce external mass transfer limitations. Thus, the factors involved in this study are the type of catalyst, reaction temperature that varied between 250^{o}C to 280^{o}C, and pressure between 40-70 bar.The catalyst deactivation tests were performed only with the catalyst with 10% Nb.

2.5. Analysis of products

The products of the hydrogenation reactions were analyzed by gas chromatography in Shimadzu equipment, model GC-2010 with flame ionization detector (FID). The samples were injected through the DB 23 column, J & W Scientific Mark.

2.6. Experimental Design and Statistical Data Analysis

The Design Expert 9.06 software was used to carry out the design. The main objective in the treatment of ANOVA data is to evaluate the influence of the interaction between the factors (temperature, pressure, and retention time), correlating their effects individually or jointly. The

factorial design was divided into two levels (2^3) with duplicate, using the experimental data of hydrogenation of palm ester. Usually, the levels of the factors are named by the signs - (minus) for the lowest level and + (plus) for the highest level, but what matters is the initial relationship between the given signal and the effect obtained, not being a defined criterion the naming of the signs. The statistical modeling of the data was restricted only to the catalyst results with 10% niobium. This catalyst presented the best conversion and selectivity results for fatty alcohols.

3.Results and Discussion

3.1.1. Nitrogen Physisorption

Table 1: Textural properties of supports and catalysts

Catalysts	Surface area -BET (m^2/g)	Pore volume (cm^3/g)	Pore Diameter (Å)
Al_2O_3	161.2	0.382	78.0
5%Nb/Al_2O_3	241.0	0.382	63.4
10%Nb/Al_2O_3	231.4	0.341	58.9
20%Nb/Al_2O_3	224.9	0.399	61.2
Re/5%Nb/Al_2O_3	210.1	0.290	55.3
Re/10%Nb/Al_2O_3	215.2	0.274	50.9
Re/20%Nb/Al_2O_3	197.8	0.290	58.7

Table 1shows the textural properties of the catalyst. The results made it evident that the impregnation of niobium in alumina allowed an increase in the surface area of the catalysts when compared to the alumina. However, volume and pore size slightly decreased. Moreover, rhenium impregnation in x%Nb/Al_2O_3led to a decrease in the catalysts' surface area, pore volume, and pore size. Similar textural properties behavior was observed in previous work [25]. For bimetallic catalysts, the slight decrease in the values of the surface area when compared to the surface areas of x%Nb/Al_2O_3may indicate that there was a certain degree of pore obstruction during the rhenium impregnation process. In contrast, the addition of Re or Ru as promoters in cobalt-based catalysts decreased their surface areas, pore volume, and pore size [26]. This behavior was attributed to the impregnation process of metals on the surface of the substrates responsible for reducing the surface area.

Furthermore, the increase in the surface area after niobium and rhenium addition may be due to the doping effect and the creation of new pores due to the effective diffusion of metals in the support [25].Niobium is stable when added to other metals in the synthesis of catalysts. The resulting catalyst's stability keeps its surface area and pore volume unchanged [27]. Other works have observed that the pore volume and the average pore diameter decrease as the Nb_2O_5 content in the catalyst increases, although, up to a certain percentage, the catalysts' surface area (BET) increases. After a certain level of niobium, the surface area decreases again [28]. The results regarding BET corroborate this work. However, the pore volume and pore diameter were different, suggesting other factors influencing the textural properties due to the addition of niobium oxide-briefly, reserve metal from the support pores [29].

3.1.2. X-Ray Diffraction (XRD)

Figure 1 shows the diffractograms of the catalysts (Re-x%Nb/Al_2O_3) and illustrates only peaks corresponding to alumina. It may indicate a better dispersion of metals (niobium and rhenium) on the alumina surface, fact-based on XPS results below.

In general, only Al2O3 diffraction peaks are observed due to the lower amount of Re and the good dispersion of Nb2O5 on the alumina surface. According to [30], the three (3) peaks of XRD of samples containing γ-alumina correspond to the separation of pairs of atoms of Al-Al, Al-O, and O-O. Any peak that appears below 1.3 Å consists of termination ripples and does not correspond to any connection length in the structure. Even varying the niobium content in the catalyst, niobium peaks were not detected. Other studies found similar results for the case of niobium [31] and rhenium [27]. After impregnating any metallic oxides, the alumina surface appears to be complementarily dehydroxylated [31].The presence of only γ-Al2O3 peaks appears to indicate that there was a better dispersion of niobium in alumina.

The lack of rhenium peaks can be related to a higher dispersion of rhenium in the supports or low content in the catalysts. According to [31], they could only detect rhenium peaks in the catalyst with a rhenium content above 10% in the catalyst; that is, it was impossible to observe any rhenium peak in proportions below this content.

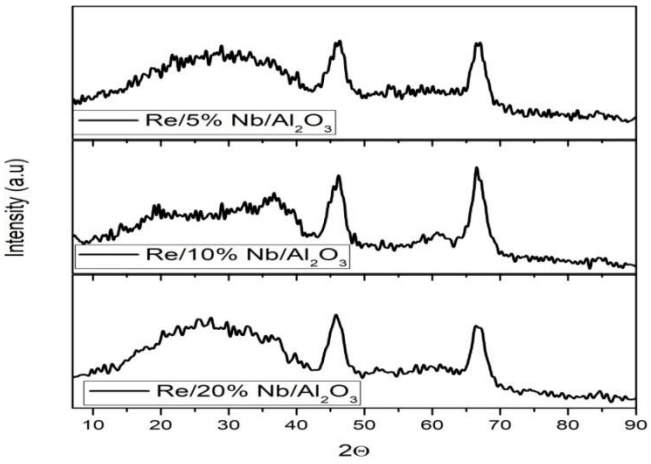

Figure 1: X-ray diffractogram of the Re-x% Nb/Al_2O_3 bimetallic catalysts

3.1.3. Temperature Programmed Reduction

Figure 2 shows the temperature-programmed reduction profiles of the catalysts. The catalyst reduction temperatures are: Re-5%Nb/Al_2O_3at 374°C, Re-10%Nb/Al_2O_3at 308.8°C and 401.2°C and Re-20%Nb/Al_2O_3at 345.2°C. The catalysts have different reduction temperatures despite being composed of the same metallic composition. This was probably due to the niobium content that varied between 5%, 10%, and 20%.

The catalyst with 10% niobium presented two reduction peaks; the second, at 401.2°C, has a higher reduction temperature when compared to the other catalysts. The peaks in the reduction temperature of the catalysts were attributed to the reduction of the Re^{7+} to Re^{0} species. Without passing through the intermediate species (Re^{+6}, Re^{+5}, and Re^{+4}).In the case of the Re-10%Nb/Al_2O_3catalyst, the two peaks would be related to the different species of Re^{7+}, being the first peak with the lowest intensity at 308.8°C corresponds to the Re^{7+} species formed by clusters; that is, the greater amount of rhenium with little interaction with the support. The second most intense peak at 401.2°C would correspond to the species in strong connection with the support. The XPS results further support the fact that the catalyst only existed with the oxidation state of Re^{7+}, as can be seen in all XPS figures (Figure 4) in the Rhenium spectra.

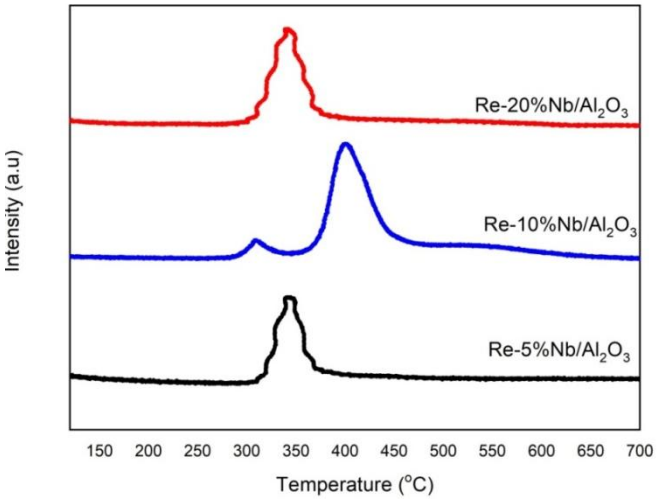

Figure 2: Profile of the Catalyst Temperature Programmed Reduction

The catalysts with 5% and 20% niobium showed low metallic dispersion of rhenium on the catalyst surface, so they presented lower reduction temperatures due to less interaction with the support. While the catalyst with 10% niobium showed more metallic dispersion of rhenium on the surface, there was a more excellent dispersion; therefore, more difficult to reduce; that is, its reduction occurs at elevated temperatures. The difference in the metallic dispersion is observed in the XPS results shown in Table 3.Contrary to what is reported in the literature and the logic indicating that lower metal content produces greater metal dispersion, metallic particles with greater metal-support interaction Toba et al. (1999). These particles must be reduced at higher temperatures. However, the TPR results do not show a definite trend with the Nb_2O_5 content.

3.1.4. Temperature Programmed Desorption

Table 2 present the acidity profiles of TPD-NH_3 of the catalysts, the values of the deconvolution areas, and the temperature ranges in which the ammonia desorption has occurred. At low temperatures, the peak deconvolutions of Re-5%Nb/$Al_2O_3$and Re-20%Nb/Al_2O_3 catalysts are found. This means that weak acidic sites mainly characterize these materials. These results corroborate the data in Table 2. The Re-10%Nb/Al_2O_3 catalyst presents the ammonia desorption profile with variation from low to high temperatures, attributed to both strongly acidic and weak acidic sites. Other studies found similar results regarding broad peaks of catalyst desorption (de Paiva et al., 2006, Jiao et al., 2016). The greatest width was attributed to different forces, both weak and strong (Bronsted acids) [34].

Table 2: Catalyst Strong/weak acid site ratio

Catalysts	µmolNH3/gcat	The ratio of acid sites (%)	
		weak	strong
Re-5%Nb-Al_2O_3	456	86, 8	13, 2
Re-10%Nb-Al_2O_3	588	76, 2	23, 8
Re-20 Nb_2O_5-Al_2O_3	579	83, 4	16, 6

The total number of acidic sites is related to the total deconvolution area generated from the TPD analysis. At the same time, the force is proportional to the temperature at which the species' desorption occurs. The stronger the acidic site, the greater the interaction with adsorbate and the higher the temperature required to remove it [35–37].

Table 2 shows that all catalysts have high acidity since the values of ammonia consumption per gram of the catalyst are high. Furthermore, only the Re-10%Nb/Al_2O_3catalyst has a large peak, also characterized by the extension of the nitrogen desorption temperature and many strong acidic sites. In contrast, Re-20%Nb/Al_2O_3catalysts showed only weak acidic sites; this probably indicates that the greater the amount of niobium oxide discharged on the surface of the alumina, the catalysts will be formed with weak acidic. The increase in acidity in the catalysts did not show any proportional relation to the increase or decrease in niobium content in the catalyst.

3.1.5. Photoelectron Spectrometer excited by X-rays (XPS)

The characterization of the catalysts by XPS aimed to determine the oxidation states of the metals Re and Nb in the Re-Nb catalysts; examine the metallic dispersion in the catalyst, and evaluate the influence of the interaction Re-Nb in the binding energies and the width of the spectra.

Figure 3 shows the adjustment curves of the XPS spectra of Re-Nb bimetallic catalysts. In catalysts, it can be seen that the rhenium has a double spectrum. The curves of the spectra revealed the presence of a doublet for all catalysts with a more intense Re 4f7/2 reference peak and the second Re 4f5/2 peak. In the same figure, it is possible to observe doubled spectra corresponding to the Nb3d species.

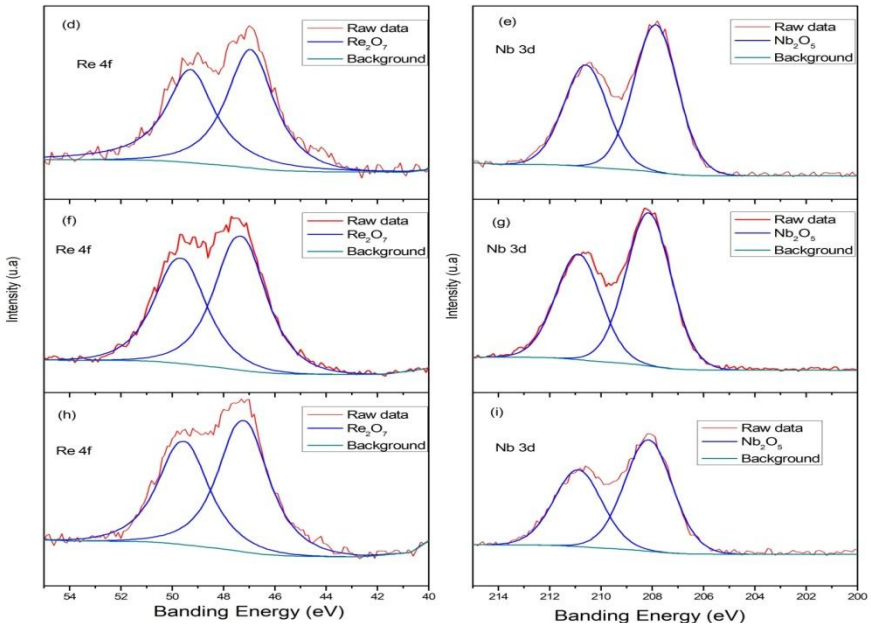

Figure 3: Rhenium XPS spectra and niobium promoter in bimetallic catalysts: (d and e) Re-5%Nb/Al_2O_3, (f and g) Re-10%Nb/Al_2O_3, and (h and i) Re-20%Nb/Al_2O_3.

The adjusted curves of both the rhenium and the Niobium spectra show a double peak for each, indicating that a single species is present for both metals. According to the graphs' profiles, niobium has binding energies in the range of approximately 208 ± 0.98, which indicates the presence of Nb^{+5} species on the support surfaceγ-Al_2O_3. These data demonstrate no reduced oxidation state of niobium (Nb^{+4} or Nb^{+3}) in these catalysts. The XPS measurements showed the binding energies with peaks between 47.1±0.9, which means the existence of the Re^{+7} species of rhenium. Therefore, the two metals did not present species from the reduced state. Similar results were obtained in previous works [38–41]. When synthesized, these researchers demonstrated that any rhenium catalyst would present a doublet before and after the reaction, regardless of the support used.

According to [42], Okal, also obtained similar results for all catalysts calcined between 500°C-800°C. The authors also found that the relative intensity and separation of the Re 4f7/2-Re5/2 rotation-orbit rotation were fixed for each doublet in the curve adjustment routine. However, the line width and position were variable to some extent. However, at temperatures below 500°C, they observed the most significant formation of Re^{4+}, Re^{6+} species. The authors believe it is indicative of a high affinity of the dispersed Re.

According to [43] from the capture of O_2 and XPS, the results showed that very small Re particles had direct and strong contact with the oxygen atoms of the support at temperatures between 20 to 500ºC. The XPS data indicated that, at room temperature, groups and small particles of rhenium were oxidized to the species Re^{4+}, Re^{6+}, and Re^{7+}. The O/Re ratios at temperatures up to 200°C increased with the Re dispersion, implying a high affinity of the highly dispersed Re to oxygen.

High temperatures accelerate the oxidation of rhenium with instantaneous sublimation of the Re_2O_7 oxide and its simultaneous adsorption as a ReO_4 species on alumina. Catalysts treated at 500ºC, regardless of the particle size of the rhenium and its interaction with the support, the total rhenium was oxidized for the Re^{7+} species (as ReO_4 groups), which is the highly dispersed surface phase of the rhenium species. These species form some type of surface complex with an Al–O–ReO_3 or Al– (O–ReO_3)$_3$ structure, which inhibits the surface migration of the rhenium and its loss by oxidized catalysts [43].The spectra of the catalysts showed no carbon on the surface or any organic molecule "COOR" that is a typical contaminating. Similar results were also obtained [44].

Table 3 presents the peak width (FWHM), atomic relationships of species on the surface, and the binding energies (BE) of the Re4f7/2 component that corresponds to the most intense spectrum for all catalysts and Nb3d5/2 of the more intense spectrum only in bimetallic catalysts.

Table 3: Summary of the binding energies of the components of rhenium and niobium, their relative properties, and their atomic relationship of the surface between Re and the %Nb/Al_2O_3.

Catalysts	Peak BE (Re4f7)	Peak BE (Nb3d5)	FWHM eV (Re4f)	FWHM eV (Nb3.)	Oxidation states of Re^{7+} ions	$^{a}_{DP}$of Nb	$^{b}_{DP}$of Re
Re-5%Nb/Al_2O_5	46.95	207.86	4.783	5.146	100%	3.42	0.62
Re-10%Nb/Al_2O_5	47.29	208.14	4.797	5.094	100%	2.68	0.94
Re-20%Nb/Al_2O_5	47.17	208.14	4.747	4.981	100%	4.52	0.75

$^{a}_{DP}$of Nb- metallic dispersion of niobium on the catalyst surface and $^{b}_{DP}$of Re –metallic dispersion of rhenium on the catalyst surface

Based on the XPS data in Table 3, the atomic concentrations of Re, Nb, and Al were obtained, and the respective atomic ratios Re/NbAl (metallic dispersion of rhenium on the catalyst surface), Nb/Al (metallic dispersion of niobium on the catalyst surface) were calculated. In this case, the sensitivity factors of the elements that make up the Re4f7/2, Re4f5/2, Nb3d, and Al2p catalysts were considered.

As shown in Table 3, only the Re-5%Nb/Al_2O_5 catalyst showed good dispersion of niobium species on γ-Al_2O_3 (Nb/Al), considering that the 5%Nb catalysts have half the niobium content in the catalyst of 10%Nb. As for the Re-10%Nb/$Al_2O_5$and Re-20%Nb/Al_2O_5 catalysts, the metallic dispersion between Nb/Al is practically similar, considering that the catalyst with 10%Nb gave an Nb/Al ratio of 2.68 and that of 20%Nb gave Nb/Al ratio of 4.52 since the relative percentage of niobium on the surface in the catalyst of 20%Nb is twice the content of niobium in the catalyst with 10%Nb. Therefore, it can be said that the variation of the niobium content in the catalysts was independent of the variation in the atomic niobium/alumina (Nb/Al) and consequently in its dispersion.

Using the XPS technique to characterize catalysts (prepared from two different niobium precursors: complex niobium and ammonia oxalate and niobium oxalate) with different levels of niobium, it was observed that the catalysts synthesized from the complex niobium and ammonium oxalate presented Nb/Al atomic ratios similar to those obtained in our study, that is, the catalyst with 5%Nb showed more excellent metallic dispersion of niobium (Nb/Al), while the catalysts with 10%Nb and 20%Nb showed almost similar dispersion of Nb/Al, considering that the catalyst with 20%Nb has twice the amount of niobium about the catalyst with 10%Nb [44]. However, the catalyst prepared using niobium oxalate as a precursor presented the oxide dispersion of the catalyst with 10% greater than the catalyst with 20%. However, the 5% catalyst shows greater metallic dispersion than those mentioned above [45].

The metallic dispersion of niobium on the surface of the catalysts depends on the charge. According to [28], for catalysts with low niobium charge, the niobium species were well dispersed in the γ-Al_2O_3 nanofiber through Nb-O-Al bridge bonds. This result is in line with our results. The metallic dispersion of rhenium in the catalysts increases in the following order: Re-10%Nb/Al_2O_3>Re-20%Nb/Al_2O_3>Re-5%Nb/Al_2O_3. According to [46], the increase in the atomic relationship in the Re/Al_2O_3 catalyst obtained through XPS analysis with the loading of completely oxidized samples suggests the presence of well-dispersed metal surface species.

The values of binding energies in Table 3 samples for Re 4f species show slight differences between them, but all correspond to the Re_2O_7 oxide with Re^{7+} oxidation status. Differences in charges of niobium content may have caused the small displacement of the binding energies. The binding energy results of both Re 4f7/2 and Nb 5d3/2 are independent of the variation of the niobium content in the catalysts. Similar results were obtained in some studies [42, 47]. However, some studies found that the binding energy was considered dependent on the size of the particles, increasing by about 0.5 eV, since the size of the particles decreases from 5 to 1 nm [48]. The analysis of the oxygen spikes as a function of the variation in the niobium content showed that the catalysts overlap the energy binding spectrum of metals and support, as shown in Table 4.

Table 4: Binding energies of the O1s components, their comparable properties, and their atomic relationship of the surface with the other components

Catalysts	Name	Peak BE (eV)	FWHM (eV)	Area (P) CPS (eV)	Atomic Reason (%)
Re5%Nb-Al	O1s A	531.46	2.345	50103.65	72.9
	O1s B	533.05	2.404	18620.61	27.1
Re10%Nb-Al	O1s A	531.67	2.404	64135.47	77.89
	O1s B	533.08	2.404	18199.87	22.11
Re20%Nb-Al	O1s A	531.56	2.294	56194.19	77.06
	O1s B	533	2.403	16727.16	22.94

The chemical oxygen environment (O1s) showed variable proportions than the expected proportions of O1s oxygen (Rhenium Oxygen 531 eV, Alumina Oxygen is 533 eV, Niobium Oxygen 529 eV) at x%Nb/Al_2O_3 and in Re_2O_7. Due to the low amount of niobium in the catalysts, it was difficult to separate the niobium oxygen peaks from the other components of the catalysts (Rhenium Oxygen and Alumina Oxygen). However, the niobium O1s species, even though it was impossible to identify, allowed the oxygen peaks (FWHM) of the species identified to be widened in an order based on the equilibrium shift from higher to lower binding energy level, Table 4.

Although it was difficult to separate the components due to the strong overlap of the O1s signal from Re_2O_7 on O1s from other catalyst components, for all cases, it was considered that the peaks in Table 4, the first O1s A peak could correspond to that of rhenium oxygen. The second O1s B peak could correspond to the oxygen of the overlapping supports. These results agree with other studies that attributed the O1 peaks of about 530-532eV to adsorbed oxygen species, such as O, OH, or H_2O [4]. However, different results also identified the peak of O1s with a binding energy of 530 eV specific. For all the components of the catalyst [49].

The different niobium loads in the bimetallic catalysts affect the O1s spectra by decreasing the binding energies (BE) and increasing the width of the peaks (FWHM), indicating that there was O1s coupling of the catalyst components. The FWHM values are higher for the spectra of the Re4f species and for the Nb3d species, which

means that these species are well dispersed over the surface of the supports, where the metals are contained.

The comparison of the O1s spectra for the catalysts illustrates that the niobium caused the displacement of the binding energy. The greater the amount of niobium on the catalysis was, the greater the displacement for lower binding energy. The lower binding energy of niobium oxide when it enters the structure alters the electronic cloud of oxygen in that region. Consequently, based on this shift, it can be said that niobium oxide is altogether interacting with other catalyst components. As for the catalyst with 10% niobium has a displacement for less energy, less than the catalyst with 5%. This can be explained by the fact that this (Re-10%Nb/Al_2O_3) has a lower niobium charge on the surface, that is, a lower atomic ratio, when compared to the Re-5%Nb_2O_5/Al_2O_3 as illustrated in Table 4 and previously described. In this logic, the equilibrium shift from higher to lower energy level follows the following sequence: Re-10%Nb/Al_2O_3<Re-5%Nb/Al_2O_3<Re-20%Nb/Al_2O_3.

Infrared Spectroscopy with Fourier Transform of Pyridine

Figure 4 shows the FTIR profile of pyridine for bimetallic catalysts. The profile of the graphs in Figure 4 shows the existence of bands at 1445 cm-1, 1490 cm-1, 1609 cm-1, 1537 cm-1, and 1640 cm-1 for all catalysts. According to the literature, bands corresponding to Lewis acid sites are found at 1445 cm-1 and 1609 cm-1, while Bronsted acid sites are found at 1537 cm-1 and 1640 cm-1. The band at 1490 cm-1 refers to both Lewis and Bronsted sites [50, 51].

According to the profile in Figure 4, the catalyst with 5%Nb had more Lewis acid sites. However, it also presents a lower intensity band of a mixture of Lewis and Bronsted acid sites. The catalyst with 10%Nb also showed a higher intensity band of Lewis acid sites and Lewis and Bronsted mixture when compared to catalysts with 5%Nb and 20%Nb. Nevertheless, some bands indicate the presence of Bronsted acid sites in the 10%Nb catalyst. The catalyst with 20%Nb had both Bronsted acid sites and Lewis acid sites; however, a smaller amount of Bronsted acid sites than in the catalyst with 10%Nb, but higher than in the catalyst with 5% Nb. Regarding the Lewis acid sites, the catalyst with 20%Nb has a smaller amount of Lewis acid sites when compared to the catalysts with 5%Nb.

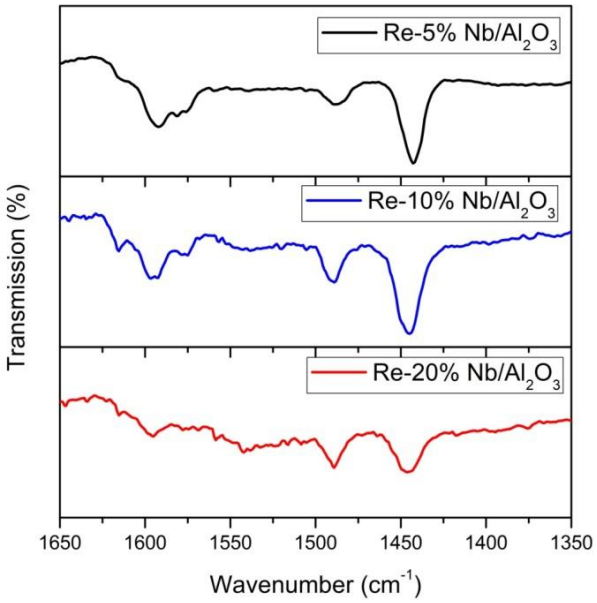

Fig. 4: Spectra of bimetallic catalysts produced from FTIR transmission of pyridine

According to [52], Lewis acid sites can be detected in all niobium catalysts, regardless of the charge. However, the strength of these acidic sites increases with Nb content. Meanwhile, Brønsted acidic sites are only found for Nb loads above 4.5%Nb, and a correlation between polymeric Nb species and the presence of Brønsted acidic sites is observed. The authors detected acidic Brønsted sites for the sample with the highest Nb surface coverage at a 9.0% charge.

3.2. Catalytic Tests

The catalytic results of the hydrogenation of palm esters are presented in Table 5 and Figure 6.

Table 5: Conversion and selectivity data for hydrogenation reactions using Re-5%Nb/Al_2O_3 catalyst

Stard order	Factor 1 Temperature (°C)	Factor 2 Time (hs)	Factor 3 Hydrogen pressure (bar)	Response 1 Conversion (%)	Response 2 Fatty Alcohol (%)	Response 2 Hydrocarbon (%)	Response4 Wax ester (%)
1	250	8	40	37.9	33.0	0	67.0
2	250	8	40	33.2	27.4	0.1	72.4
3	280	8	40	41.6	18.5	0	81.5
4	280	8	40	42.0	19.9	0	80.1
5	250	10	40	55.0	11.0	0	89.0
6	250	10	40	51.9	14.7	0	85.4
7	280	10	40	63.5	19.2	0.2	80.6
8	280	10	40	68	23.1	0	76.9
9	250	8	70	39.7	19.1	0	80.9
10	250	8	70	40.1	17.7	0.8	81.5
11	280	8	70	86.5	19.3	0.6	80.0
12	280	8	70	83.3	22.1	1.0	76.9
13	250	10	70	59.3	16.0	0.1	83.7
14	250	10	70	63.1	20.5	1.0	78.5
15	280	10	70	86.9	29.0	3.2	67.7
16	280	10	70	89.7	33.0	2.9	64.1

Table 5 shows that the catalyst with 5% niobium indicated that the three factors influenced the conversion of esters. The higher the temperature, pressure, and residence time, the greater the conversion. However, the selectivity of products, especially fatty alcohols, was not proportional to all reaction conditions. The best selectivity of fatty alcohols, which was 33.0%, was achieved using 250°C, 8h, and 40 bar and 280°C, 10 h, and 70 bar, which means that the variation in conditions was not so influential in obtaining the highest fatty alcohol yield, which is a product of interest. However, the temperature and residence time can be constant. The temperature influenced the selectivity of the products in general; that is, the reactions carried out at 250°C and 40 bar at 8h had a higher selectivity of fatty alcohols than the reactions under the same conditions but the temperature of 280°C. However, it is essential to note that despite this selectivity behavior, the reactions carried out at a temperature of 280°C have consistently shown more excellent conversion than the reactions carried out at 250°C. Furthermore, in the same reactions analyzed above, when the residence time is increased from 8h to 10h, it is observed that the fatty alcohol yield decreases a little due to the favoring of the reaction for the formation of wax esters.

The reactions carried out at 280°C, and 70 bar indicate no significant change in the yield of fatty alcohols, regardless of the variation of the factors. In general, Table 5 illustrates a favorable production of wax esters regardless of the conditions applied in the reactions. Additionally, the lower conditions 250°C and 40 bar, did not favor the formation of hydrocarbons, but at temperatures of 280°C and 70 bar, there were traces of hydrocarbons.

The wax esters are the intermediate with the highest selectivity in reactions. This selectivity of wax esters as an intermediate was that they are the slowest step in the process. When evaluating this behavior of the products as a function of temperature and pressure variation, it can be seen that it may be due to thermodynamic reasons. There is a low formation of wax esters at low pressures and temperatures, probably due to low conversion. In contrast, there is a greater formation of wax esters and conversion at high temperatures and low pressures. High-pressure reactions show a higher rate of conversion of esters and then wax esters to fatty alcohols at 280°C compared to 250°C. The reaction in a heterogeneous medium may also be fundamental to justify the slow conversion rate of wax esters into fatty alcohols, as previously discussed. The reactions were carried out in a heterogeneous medium because one of the objectives was to avoid using organic solvents.

Table 6: Conversion and selectivity data for hydrogenation using Re-10%Nb/Al2O3 catalyst

Stard ordem	Fator 1 Temperature (oC)	Fator 2 Time (hs)	Fator 3 Hydrogen pressure (bar)	Response 1 Conversion (%)	Response2 Fatty Alcohol (%)	Response 3 Hydrocarbon (%)	Response4 Wax ester (%)
1	250	8	40	32.01	40.62	0	59.38
2	250	8	40	27.83	41.41	0.53	58.06
3	280	8	40	73.21	34.69	1.12	64.19
4	280	8	40	66.02	29.03	0.2	70.77
5	250	10	40	46.91	34.11	0	65.89
6	250	10	40	39.97	35	0	65
7	280	10	40	76.98	45.63	1.15	53.22
8	280	10	40	75.69	47.05	1.07	51.88
9	250	8	70	70	34.82	1.62	63.56
10	250	8	70	67.83	35.9	0	64.01
11	280	8	70	84.28	61.12	0	38.88
12	280	8	70	85.11	63	0.21	36.79
13	250	10	70	88.64	46.29	1.89	51.82
14	250	10	70	83.62	49	0.84	50.16
15	280	10	70	88.32	75.02	2.48	22.5
16	280	10	70	91.08	78.64	2.76	18.6

Results in Table 6 show that 10% niobium catalyst has a different activity from the 5% niobium catalyst in the reactions carried out at 40 bar pressure. That is, reactions carried out at 40 bar at a temperature of 250°C show low conversion during 8h of reaction. However, the selectivity of fatty alcohols is greater than the same reaction with 10 hours of reaction—however, the conversion increases at a longer reaction time. The low conversion to fatty alcohols in 10 hours of reaction, when compared to 8 hours of the reaction observed for reactions carried out with 250°C and 40 bar, was due to the formation of wax esters, which were probably the result of the reaction of fatty alcohols already produced with the raw material of process.

The reactions carried out at 280°C obtained a better conversion of palm esters and selectivity of fatty alcohols when compared to the reactions carried out at 250°C under the same pressure conditions. It is important to note that in reactions carried out at 280°C, the conversion and selectivity of fatty alcohols increase with longer the reaction time. This may mean that the kinetic balance of the reaction favors the production of fatty alcohols, reducing the shape of the intermediate (wax esters).As for the formation of hydrocarbons (unwanted products), a result similar to that illustrated in table 5 was obtained. Reactions at temperatures of 280°C favor the production of hydrocarbons. As mentioned in the literature, the low formation of hydrocarbons is favored by thermodynamic conditions and the catalyst (rhenium) [3, 14].

Table 7: Conversion and selectivity data for hydrogenation using Re-20%Nb/Al_2O_3 catalyst

Stard order	Factor 1 Temperature (oC)	Factor 2 Time (hs)	Factor 3 Hydrogen pressure (bar)	Response1 Conversion (%)	Response2 Fatty Alcohol (%)	Response3 Hydrocarbon (%)	Response4 Wax ester (%)
1	250	8	40	27.7	26.3	0	73.7
2	250	8	40	23.9	28.1	0	71.9
3	280	8	40	68.4	9.9	0	90.1
4	280	8	40	68	10.2	0	89.9
5	250	10	40	30.5	24.8	0	75.2
6	250	10	40	31.0	25.5	0	74.5
7	280	10	40	71.1	13.6	1.0	85.4
8	280	10	40	69.5	16.2	0	83.8
9	250	8	70	38.2	19.6	0	80.4
10	250	8	70	37.8	21.0	0.0	79.0
11	280	8	70	70.9	18.7	0.8	80.5
12	280	8	70	72.1	20.7	1.0	78.9
13	250	10	70	43.5	20.9	0	79.2
14	250	10	70	45.1	23.3	0.4	76.3
15	280	10	70	71.7	21.5	1.2	77.3
16	280	10	70	74.4	22.4	2.2	75.3

The catalyst with 20% shows similar results to those presented with the catalyst with 5% niobium regarding the conversion and selectivity towards fatty alcohols. These two catalysts showed a low yield in the production of fatty alcohols compared to the 10% niobium catalyst, with an average of 89.7 % palm esters conversion duplicate which resulted in 76.8% selectivity in fatty alcohols. This result was achieved at 280^{o}C and 70 bar of hydrogen during 10 hours of reaction. Catalysts with 5% and 20% niobium content may have obtained similar results as both have weak acidic sites compared to the catalyst with 10% niobium content; this agrees with the results obtained TPD-NH_3. On the other hand, according to the XPS results, these two catalysts show a lower dispersion of the rhenium in the catalyst, as previously described.

In general, the conversion and selectivity results illustrated in the three Tables 5, 6, and 7 show that the reactions carried out at 280^{o}C and 70 bar showed promising results. This trend indicates that the combination of higher pressure and temperature favors more excellent catalytic activity and improves the yield and selectivity of the desired product and the conversion of palm esters. The catalysts showed similar behavior regarding the conversion and selectivity of the products. The three catalysts demonstrated higher temperature (280^{o}C), the increased conversion rate of palm ester, and selectivity towards fatty alcohols, except in some cases where there was the production of traces of hydrocarbons. At temperatures of 250^{o}C, the conversion decreased while the selectivity of fatty alcohol increased.

The results also show reaction intermediates (wax esters) production in all systems that increase their selectivity with the increased time of the reaction and simultaneously convert them into fatty alcohols [8, 58]. However, only the rate of formation of the intermediates is fast. However, their transformation into fatty alcohols is not flexible under certain operational conditions, especially for reactions without the solvent. This is a different important factor compared to other studies in the literature. Our results corroborate with the results found by other works that found the total conversion of esters and formation of intermediates to be faster. At the same time, the reaction continued to take longer for the intermediates to be converted into the final product [53].

Based on the results, it can be concluded that the equilibrium constant of the ester hydrogenolysis reaction for the production of fatty alcohols increases with increasing system temperature. In thermodynamic terms, this reaction must be carried out at not too high temperatures to increase the selectivity of fatty alcohols and avoid the formation of hydrocarbons, as seen in the reactions at 280^{o}C, where there was the production of traces of hydrocarbons (C16 and C18).

Comparing the activity of the three (3) catalysts, the catalyst with 10% niobium showed better conversion and selectivity when compared with the other catalysts with 5% and 20% niobium. The activity of the catalysts increases in the order of Re-10% Nb/Al_2O_3> Re-20%Nb/Al_2O_3> Re-5%Nb/Al_2O_3. The difference in the activity of the catalysts can be justified by the metallic dispersion of rhenium, whereby the catalyst with 10% niobium was the one with the greatest dispersion, followed by the catalyst with 20% niobium. This dispersion was strongly supported by XPS data (Figure 4) in the atomic ratio of rhenium on the catalyst surface.

Rhenium is one of the few metals highly active in this reaction. Its catalysts are promising for partially removing oxygen from oils and their derivatives by producing alcohol in the corresponding carbon chain [3, 21]. Considers that the effectiveness of the monometallic rhenium catalyst for the production of fatty alcohols can be improved with the addition of co-catalyst, mainly of noble metals (ruthenium, rhodium, platinum, and palladium). Several studies indicate that certain metals as promoters in hydrogenolysis reactions increase the yield and selectivity of fatty alcohols and simultaneously reduce the production of unwanted products, for example, the Zinc and Cobalt, co-catalyst [54]; tin [32]. According to [32], tin as a co-catalyst influences the distribution of the products meaning tin controls the adsorption of the substrates and the reactivity of the functional groups of the

substrates. [54] demonstrated that in most cases, adding a co-catalyst increases the selectivity of fatty alcohols. However, there are metals (Zn and Co) that, when added, do not favor the formation of fatty alcohols despite increasing the catalytic activity of the process.

Based on the ammonia TPD results, the catalyst with Re-10%Nb/Al_2O_3 showed more strong acid sites than the other catalysts with 5%Nb and 20% Nb. That is greater acid strength, which exercised an essential role in converting esters, mainly in the selectivity of fatty alcohols. This acidic force may indicate the presence of Bronsted's acidic sites on the metal surface. Bronsted acidic sites may have been responsible for the better catalytic performance of this catalyst. According to [55], the Lewis acidic sites resulting from the formation of catalysts are generally weaker than those initially present in the oxide supports. The TPD results of the 5%Nb and 20%Nb catalysts showed the presence of weak total acid sites. These two catalysts probably had a higher amount of weak Lewis acid sites. The lower amount of niobium in the catalysts has more Lewis acid sites. The ratio of Lewis acidic sites decreases with an increase in niobium content, and in parallel, there is a formation of Bronsted acidic sites [45, 55, 56]. According to [52], the better catalytic performance is mainly due to the strength of the acid sites and the presence of Brønsted acid sites, with catalysts having stronger acid sites and a more significant number of Brønsted acid sites being more active.

According to [55], when studying the acidity of various oxides, they identified Lewis acid sites in all catalysts. However, Bronsted acid sites were obtained only Nb/Al_2O_3catalysts and Nb/SiO_2. The authors associated Bronsted's acidity with the creation of bridged hydroxyls formed between the surfaces of niobium oxide species and the alumina support.

The interaction between the Nb_2O_5 precursor and the γ-Al_2O_3 nanofiber results in niobium species with strong Lewis acidic and intense Brønsted acidic sites. While the increasing the Nb_2O_5 load led to the formation of two-dimensional polymerized niobium species three-dimensional polymerized niobium species [28, 52]. These species significantly influenced the distribution and quantity of Lewis acid sites and Brönsted sites on Nb_2O_5-γ-Al_2O_3 nanofibers [28].

Bronsted's acidic sites appear, and the monolayer form-critical surface coverage of the supported niobium oxide species. This monolayer increases with increased superficial coverage (increased niobium load) and reaches its maximum before the monolayer is covered. Therefore, there is a direct relationship between critical concentration and surface metal oxide species [55].Some studies characterizing the catalysts of 5%Nb/Al_2O_3, 10%Nb/Al_2O_3, and 20%Nb/Al_2O_3 using the pyridine infrared technique have observed that although the number of Bronsted acid sites increases with the increase in niobium content among these catalysts, the amount of Lewis acid sites is always greater with 5%Nb. This amount of Lewis acid sites decreases considerably for the 10%Nb catalysts, but in the 20%Nb catalysts, this amount of Lewis acid sites increases again [28, 45, 55]. In this context, it may be that the catalyst with 10%Nb obtained the best result because the appropriate ratio between the Lewis acid sites and the Brönsted acid sites is more appropriate and, therefore, adequate to improve the dispersion of rhenium as shown by the XPS results.

All niobium catalysts can detect Lewis acid sites, regardless of the charge. Meanwhile, Brønsted acid sites are found only for Nb loads above 4.5%Nb, and a correlation is observed between polymeric Nb species and the presence of Brønsted acid sites. The authors were able to detect Brønsted acid sites for the sample with the highest Nb surface coverage with a 9.0% load. For [57], niobium oxide catalysts prepared from niobium oxalate as a precursor present in their surface phase two types of niobium oxide species in the alumina support. Their relative concentrations depend on their relative concentrations of the coverage of niobium oxide. The presence of surface phases of niobium oxide not only slows down the loss in the surface area but also the surface niobium oxide species in the support has a strong Bronsted acidity [57, 58].

3.3. Catalyst deactivation tests

Results in Figure 5 illustrate that the catalyst suffered a slight reduction in its activity over time, not only due to the difference between the conversions of the three reactions (fresh-reduced catalyst and the two reuses), which are statistically similar but also due to the selectivity of fatty alcohols. As seen in the first reuse reaction, the conversion difference with the fresh catalyst reaction was minimal. The degree of selectivity decreased by approximately 11% compared to the reaction that used the fresh catalyst in the second reuse step, but the conversion reduced slightly. The decrease in the selectivity of fatty alcohols favored the formation of wax esters, which means that the catalyst was getting deactivated, causing a slower rate of conversion of wax esters to fatty alcohols,

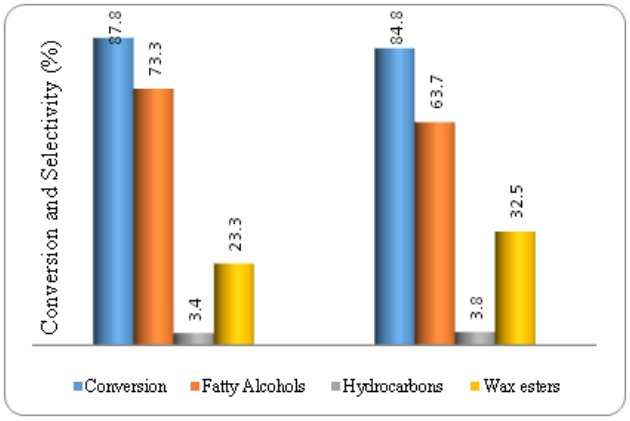

Figure 5: Ester conversion and product selectivity during Re-10%Nb/Al_2O_3 catalyst deactivation tests

Several possible contaminants during the production of fatty alcohols through the hydrogenation of both fatty acids and fatty acid esters have already been studied [19, 53, 58]. However, the existence of possible contaminants

(traces of glycerin, free fatty acids, phosphates, chlorides, etc.) was not analyzed. A possible catalyst contaminant may be the reaction intermediate itself (wax esters) and the possible existence of free fatty acids in the raw material. Water can interfere with the activity of the catalyst since when it is present in the liquid phase of the reaction; it can effectively block the active sites of the catalyst by occlusion. According to [59], the hydrogenation of methyl ester using Cu-Cr catalyst with different levels of water during feeding found that the greater the amount of water added in the process allowed effective blocking of the catalyst's active sites periodically. However, even though water does not obstruct the active sites of the catalysts, the results showed that it could inhibit the reduction of the catalysts to their active form of zero valences. Some catalysts in hydrogenolysis reactions can be considered temporary poisons to water like soaps, fatty acids, glycerin, and glycerides in the deactivation process. This can be attributed to some permanent poisons from these reactions, including halogens, sulfur, or phosphorus. Although this study was developed with a Cu-Cr catalyst, there is a likelihood that these poisons will affect other types of catalysts.

3.4. Experimental modeling and statistical analysis of data

3.4.1. Regression model equations

The experimental data were analyzed using the analysis of variance (Moreno, Ramirez-Reina, et al.) in all regression models (linear, interaction of 2FI factors, polynomial, quadratic and cubic). The quadratic model and factor interaction (2FI) were the most suitable models to calculate the significance and representation of the regression for each evaluated experimental response and its interactions. The model equations are based on the coded values (A, B, and C, represented by temperature, pressure, and retention time).

Final Equation in Terms of Coded Factors:

Conversion =+68.59 +11.49*A +5.31*B +13.77*C -2.38 *A* B -6.66 *A*C +0.25*B*C (1)

Final Equation in Terms of Coded Factors:

Fatty Alcohol = +46.96 +7.31*A +4.38*B +8.52*C +2.93 *A*B +6.66*A*C +2.38*B*C (2)

The two coded equations in the model confirm the fact previously interpreted that all factors (temperature, pressure, and retention time) are affluent in the reaction. Both in the conversion of the substrate and the formation of fatty alcohols, the influencing power of the factors and their interactions grows in the following logic: temperature (A)> pressure (B)> retention time (C)> AB> AC> BC.

3.4.2. Analysis of Variance

Table 8 shows the results of the analysis of variance. The P-value associated with the test-F statistic (P-value = 0.0149) observed in the ANOVA table suggests that, at a significance level of 95% (α = 0.05), the hypothesis that the factors individually and jointly do not affect the conversion of palm esters, that is, the model is statistically significant. Although the model hypothesis tests and the factors temperature, pressure, retention time, and their interactions are statistically significant, the lack of fit test, which represents the lack of fit in the regression model, was not adequate; that is, it is not statistically significant.

Table 8: Analysis of variance for the conversion of esters

Response	**1**	**Conversion**			
ANOVA for selected factorial model					
Analysis of variance table [Partial sum of squares - Type III]					
	Sum of		Mean	F	p-value	
Source	Squares	df	Square	Value	Prob > F	
Model	6396.058	6	1066.01	111.6591	< 0.0001	High significant
A-Temperature	2113.241	1	2113.241	221.3512	< 0.0001	High significant
B-Time	450.7129	1	450.7129	47.20988	< 0.0001	High significant
C-Pressure	3032.154	1	3032.154	317.6027	< 0.0001	High significant
AB	90.34503	1	90.34503	9.463182	0.0132	significant
AC	708.6244	1	708.6244	74.2248	< 0.0001	High significant
BC	0.9801	1	0.9801	0.10266	0.7560	Not significant
Residual	85.92303	9	9.547003			
Lack of Fit	7.317025	1	7.317025	0.744679	0.4133	not significant
Pure Error	78.606	8	9.82575			
Cor Total	6481.981	15				
Std. Dev.	3.089822		R-Squared	0.986744		
Mean	68.59375		Adj R-Squared	0.977907		
C.V. %	4.504525		Pred R-Squared	0.958106		
PRESS	271.5592		Adeq Precision	29.91229		

For the conversion of esters, the ANOVA table indicates that the model and the three factors (temperature, time, and pressure) are highly significant (all with values of p <0001). Certainly, this fact was evident in Table 6, where high temperatures (280°C) influenced the increase of esters conversion. Low temperatures, especially at low hydrogen pressures (40 bar). A similar effect was observed with the action of pressure and retention time factors, that is, the higher the pressure (70 bar) and the retention time (10h), but it was the conversion of palm

esters into products and by-products in comparison with low pressures (40 bar and 8 h) respectively.

Table 9: Analysis of variance for the formation of fatty alcohols

Response	2	Fatty alcohol			
ANOVA for selected factorial model					
Analysis of variance table [Partial sum of squares - Type III]					
	Sum of		Mean	F	p-value	
Source	Squares	Df	Square	Value	Prob > F	
Model	3260.608	6	543.4347	42.36188	< 0.0001	High significant
A-Temperature	856.0013	1	856.0013	66.72711	< 0.0001	High significant
B-Time	307.5639	1	307.5639	23.97525	0.0009	Significant
C-Pressure	1160.254	1	1160.254	90.44424	< 0.0001	High significant
AB	137.1827	1	137.1827	10.69368	0.0097	Significant
AC	709.0238	1	709.0238	55.2699	< 0.0001	High significant
BC	90.58281	1	90.58281	7.061121	0.0262	Significant
Residual	115.4555	9	12.82839			
Lack of Fit	85.14676	1	85.14676	22.4745	0.0015	Significant
Pure Error	30.30875	8	3.788594			
Cor Total	3376.064	15				
Std. Dev.	3.581674		R-Squared	0.965802		
Mean	46.95813		Adj R-Squared	0.943003		
C.V. %	7.627379		Pred R-Squared	0.891917		
PRESS	364.8964		Adeq Precision	18.98225		

The coefficients of determination (R^2), referring to both the conversion of palm esters and the selectivity of fatty alcohols (Tables 8 and 9), are explained by the variations of all factors (pressure, temperature, and retention time). The factors affect 98.40% of the conversion of palm esters and 96.6% of the selectivity of fatty alcohols, which means that the factors are adequate to explain the behavior of the results obtained. Furthermore, the coefficients of determination in the conversion and selectivity of alcohols show that the experimental values are close to the adjusted R^2 and the predicted R^2, which demonstrates good agreement between the experimental and predicted values, as shown in Figure 6.

Figure 6: Predicted values versus actual values of the experimental responses, with a) conversion of palm esters and b) selectivity of fatty alcohols.

As the predicted vs. Actual graphs illustrate, the model is statistically valid since the residual distribution or error term is normal. All points are along the axis of the centerline for the Predicted vs. Current graphs in Figure 6.

3.4.3. Study of reaction parameters

The model presents adequacy of the adjusted data between the predicted values VS current both in the conversion and in the selectivity of the fatty alcohols according to the three independent variables (temperature, pressure, and time), and the final adjusted models obtained considered for construction of Figures 7 and 8 of 3D response surface corresponding to the conversion of esters and selectivity of fatty alcohols respectively.

Figure 7: Effect of factors (A: temperature, B: Retention time, and C: H_2 pressure) on the conversion of palm esters: (a) A plot of the surface response with a pressure of 70 bar, (b) A plot of the surface response with the pressure of 40 bar.

Graphs a) and b) of Figure 7 shows the temperature variation as a function of time, considering the constant pressure (graph a) the constant pressure was 70 bar, while in graph a) the pressure constant reaction was 40 bar. From the Analysis in Figure 8, the influence of pressure becomes evident by looking at the two graphs that indicate that the best maximum conversion was achieved at the upper limits of the three factors under study.

Figure 8:
Effect of factors (A: temperature, B: Retention time, and C: H_2 pressure) on fatty alcohol selectivity: (a) A plot of the surface response at a pressure of 70 bar, (b) A plot of the surface response with a pressure of 40 bar.

In the conversion graphs in Figure 8, in the selectivity of fatty alcohols, the highest yield of molar selectivity of fatty alcohols was achieved at high temperatures (280^{o}C) and pressures (70 bar), obviously with a reaction time of 10h, that is, it was evident that the three factors have a positive influence on the selectivity of fatty alcohols.

3.4.5. Optimization of the conversion and selectivity of fatty alcohols

The Optimization of the process was fundamental for deciding which factors favor the conversion of esters and selectivity of fatty alcohols. For this, information on the influence of factors (temperature, pressure, and retention time) and their interactions was very fundamental. Therefore, based on the experimental results, the software considered optimal conditions to be the process of 280^{o}C of temperature, 70 bar of pressure, and 10 hours of retention time. Under these conditions, the maximum expected conversion was 90.37% and 79.13% selectivity. Therefore, the experimental results show an excellent precision and repeatability of approximately 99.44%.

4.Conclusion

The results obtained through hydrogenolysis suggest a good performance of the catalysts. The catalyst Re-10%Nb/Al_2O_3, in particular, obtained the best catalytic activity and highest yield of fatty alcohols. The higher activity obtained from the Re-10%Nb/Al_2O_3 catalyst corroborates the result of XPS, where the catalyst presented higher metallic dispersion compared with the other catalysts. From TPR profiles, there was a peak of reduction of rhenium in all catalysts, except for the Re-10%Nb/Al_2O_3 catalyst, which had two peaks. These peaks were attributed to the reduction of Re^{7+} to Re^0 species, a fact confirmed by XPS analysis.

The results of TPD also showed that the acid strength was necessary for the catalytic performance of the catalysts. So, the highest observed acid strength of the 10%Nb catalyst exercised an essential role in the selectivity for fatty alcohols. Temperature, pressure, and reaction time were fundamental factors in the process since higher temperature (280ºC), pressure (70bar), and retention time (10h) resulted in a higher conversion of palm esters and selectivity towards fatty alcohols. Low temperature,

pressures, and retention time generally favored the formation of intermediate products (wax esters) with greater selectivity and low conversion. The catalyst deactivation tests showed specific stability of the catalysts, maintaining conversion and selectivity. However, the stability starts to drop, in terms of selectivity, in the third reuse of the catalyst. This deactivation was probably due to tractions of free fatty acids from the raw material and water resulting from the dehydration of fatty alcohols, blocking the catalyst's active sites by occlusion. Thermodynamic reasons account for the slow conversion rate of wax esters to fatty alcohols for most reactions.

Acknowledgment

The authors thank Capes and INCT-Midas for their financial support and EPQB (Programa de Engenharia de Processos Químicos e Bioquímicos)/UFRJ

References

[1] R. Loe, E. Santillan-Jimenez, M. Crocker, Upgrading of Lipids to Fuel-like Hydrocarbons and Terminal Olefins via Decarbonylation/Decarboxylation, in: Chemical Catalysts for Biomass Upgrading, Wiley, 2020: pp. 497–528. https://doi.org/10.1002/9783527814794.ch12.

[2] D.H. Nguyen, G. Raffa, Y. Morin, S. Desset, F. Capet, V. Nardello-Rataj, F. Dumeignil, R.M. Gauvin, Solvent- and base-free synthesis of wax esters from fatty acid methyl esters by consecutive one-pot, two-step catalysis, Green Chemistry. 19 (2017) 5665–5673. https://doi.org/10.1039/c7gc02764h.

[3] B. Rozmysłowicz, A. Kirilin, A. Aho, H. Manyar, C. Hardacre, J. Wärnå, T. Salmi, D.Y. Murzin, Selective hydrogenation of fatty acids to alcohols over highly dispersed ReOx/TiO2 catalyst the paper is dedicated to the living memory of Dr. Haldor Topsøe., Journal of Catalysis. 328 (2015) 197–207. https://doi.org/10.1016/j.jcat.2015.01.003.

[4] T. Toyao, K.W. Ting, S.M.A.H. Siddiki, A.S. Touchy, W. Onodera, Z. Maeno, H. Ariga-Miwa, Y. Kanda, K. Asakura, K. ichi Shimizu, Mechanistic study of the selective hydrogenation of carboxylic acid derivatives over supported rhenium catalysts, Catalysis Science and Technology. 9 (2019) 5413–5424. https://doi.org/10.1039/c9cy01404g.

[5] K. Kandel, U. Chaudhary, N.C. Nelson, I.I. Slowing, Synergistic Interaction between Oxides of Copper and Iron for Production of Fatty Alcohols from Fatty Acids, ACS Catalysis. 5 (2015) 6719–6723. https://doi.org/10.1021/acscatal.5b01664.

[6] T. Voeste, H. Buchold, Production of fatty alcohols from fatty acids, J Am Oil Chem Soc. 61 (1984) 350–352. https://doi.org/10.1007/BF02678794.

[7] K. Noweck, W. Grafahrend, Fatty Alcohols, in: Ullmann's Encyclopedia of Industrial Chemistry, Wiley-VCH Verlag GmbH & Co. KGaA, Weinheim, Germany, 2006. https://doi.org/10.1002/14356007.a10_277.pub2.

[8] D.S. Thakur, A. Kundu, Catalysts for Fatty Alcohol Production from Renewable Resources, JAOCS, Journal of the American Oil Chemists' Society. 93 (2016) 1575–1593. https://doi.org/10.1007/s11746-016-2902-x.

[9] L. Wu, L. Li, B. Li, C. Zhao, Selective conversion of coconut oil to fatty alcohols in methanol over a hydrothermally prepared Cu/SiO2 catalyst without extraneous hydrogen, Chemical Communications. 53 (2017) 6152–6155. https://doi.org/10.1039/c7cc01126a.

[10] A. Ali, B. Li, Y. Lu, C. Zhao, Highly selective and low-temperature hydrothermal conversion of natural oils to fatty alcohols, Green Chemistry. 21 (2019) 3059–3064. https://doi.org/10.1039/c9gc01260e.

[11] N.W. Cant, D.L. Trimm, The Catalytic Hydrogenolysis of Esters to Alcohols, Catalysis Reviews. 36 (1994) 645–683. https://doi.org/10.1080/01614949408013931.

[12] J.E. Carnahan, T.A. Ford, W.F. Gresham, W.E. Grigsby, G.F. Hager, V. 77, C.C. Price, D.C. Lincoln, Ruthenium-catalyzed Hydrogenation of Acids to Alcohols, 1951. https://pubs.acs.org/sharingguidelines.

[13] X. Cui, Y. Li, C. Topf, K. Junge, M. Beller, Direct Ruthenium-Catalyzed Hydrogenation of Carboxylic Acids to Alcohols, Angewandte Chemie - International Edition. 54 (2015) 10596–10599. https://doi.org/10.1002/anie.201503562.

[14] H.G. Manyar, C. Paun, R. Pilus, D.W. Rooney, J.M. Thompson, C. Hardacre, Highly selective and efficient hydrogenation of carboxylic acids to alcohols using titania supported Pt catalysts, Chemical Communications. 46 (2010) 6279–6281. https://doi.org/10.1039/c0cc01365j.

[15] M. Martinelli, R. de C. de S. Schneider, V.Z. Baldissarelli, M.L. von Holleben, E.B. Caramao, Castor oil hydrogenation by a catalytic hydrogen transfer system using limonene as hydrogen donor, J Am Oil Chem Soc. 82 (2005) 279–283. https://doi.org/10.1007/s11746-005-1067-4.

[16] B. Rozmysłowicz, P. Mäki-Arvela, A. Tokarev, A.R. Leino, K. Eränen, D.Y. Murzin, Influence of hydrogen in catalytic deoxygenation of fatty acids and their derivatives over Pd/C, in: Industrial and Engineering Chemistry Research, 2012: pp. 8922–8927. https://doi.org/10.1021/ie202421x.

[17] J. Chen, COPPER CATALYST FOR DEHYDROGENATION APPLICATION, 2014.

[18] Y. Hattori, K. Yamamoto, J. Kaita, M. Matsuda, S. Yamada, Development of nonchromium catalyst for fatty alcohol production, JAOCS, Journal of the American Oil Chemists' Society. 77 (2000) 1283–1288. https://doi.org/10.1007/s11746-000-0202-6.

[19] H. Huang, G. Cao, C. Fan, S. Wang, S. Wang, Effect of water on Cu/Zn catalyst for hydrogenation of fatty methyl ester to fatty alcohol, Korean Journal of Chemical Engineering. 26 (2009) 1574–1579. https://doi.org/10.1007/s11814-009-0267-7.

[20] K. Liu, J. Pritchard, L. Lu, R. van Putten, M.W.G.M. Verhoeven, M. Schmitkamp, X. Huang, L. Lefort,

C.J. Kiely, E.J.M. Hensen, E.A. Pidko, Supported nickel-rhenium catalysts for selective hydrogenation of methyl esters to alcohols, Chemical Communications. 53 (2017) 9761–9764. https://doi.org/10.1039/c7cc04759b.

[21] B.C. Trivedi, D. Grote, T.O. Mason, Hydrogenation of Carboxylic Acids and Synergistic Catalysts, J Am Oil Chem Soc. 58 (1981) 17–20. https://doi.org/10.1007/BF02666046.

[22] W. Xu, L. Yan, H. Wang, S. Liaw, H. Luo, Niobium-doped titanium dioxide on a functionalized carbon supported palladium catalyst for enhanced ethanol electro-oxidation, RSC Advances. 7 (2017) 34618–34623. https://doi.org/10.1039/c7ra05208a.

[23] E.A. Yahya, N.A.M. Zabidi, C.F. Kait, A study on coke deposition in Ni-based catalysts for CO2 reforming of methane, in: AIP Conference Proceedings, American Institute of Physics Inc., 2016. https://doi.org/10.1063/1.4968070.

[24] Y. Zhao, X. Zhou, L. Ye, S. Chi Edman Tsang, Nanostructured Nb 2 O 5 catalysts , Nano Reviews. 3 (2012) 17631. https://doi.org/10.3402/nano.v3i0.17631.

[25] E. Tezel, H.E. Figen, S.Z. Baykara, Hydrogen production by methane decomposition using bimetallic Ni–Fe catalysts, International Journal of Hydrogen Energy. 44 (2019) 9930–9940. https://doi.org/10.1016/j.ijhydene.2018.12.151.

[26] H. Romar, A.H. Lillebo, P. Tynjala, T. Hu, A. Holmen, E.A. Blekkan, U. Lassi, H2-TPR, XPS and TEM Study of the Reduction of Ru and Re promoted Co/γ-Al2O3, Co/TiO2 and Co/SiC Catalysts, Journal of Materials Science Research. 5 (2016) 33. https://doi.org/10.5539/jmsr.v5n2p33.

[27] S. Furukawa, T. Shishido, K. Teramura, T. Tanaka, Photocatalytic oxidation of alcohols over TiO 2 covered with Nb 2O 5, ACS Catalysis. 2 (2012) 175–179. https://doi.org/10.1021/cs2005554.

[28] H. Jiao, X. Zhao, C. Lv, Y. Wang, D. Yang, Z. Li, X. Yao, Nb2O5-γ-Al2O3 nanofibers as heterogeneous catalysts for efficient conversion of glucose to 5-hydroxymethylfurfural, Scientific Reports. 6 (2016). https://doi.org/10.1038/srep34068.

[29] J. Ramírez, R. Contreras, P. Castillo, T. Klimova, R. Zárate, R. Luna, Characterization and catalytic activity of CoMo HDS catalysts supported on alumina-MCM-41, 2000.

[30] L. Samain, A. Jaworski, M. Edén, D.M. Ladd, D.K. Seo, F. Javier Garcia-Garcia, U. Häussermann, Structural analysis of highly porous γ-Al2O3, Journal of Solid State Chemistry. 217 (2014) 1–8. https://doi.org/10.1016/j.jssc.2014.05.004.

[31] M. Massa, A. Andersson, E. Finocchio, G. Busca, Gas-phase dehydration of glycerol to acrolein over Al2O 3-, SiO2-, and TiO2-supported Nb- and W-oxide catalysts, Journal of Catalysis. 307 (2013) 170–184. https://doi.org/10.1016/j.jcat.2013.07.022.

[32] M. Toba, S.-I. Tanaka, S.-I. Niwa, F. Mizukami, Z. Koppány, L. Guczi, K.-Y. Cheah, T.-S. Tang, Synthesis of alcohols and diols by hydrogenation of carboxylic acids and esters over Ru-Sn-Al 2 O 3 catalysts, 1999.

[33] J.B. de Paiva,; W R Monteiro, M.A. Zacharias, J.A.J. Rodrigues,; G G Cortez, INFLUÊNCIA DA ADIÇÃO DE MoO 3 SOBRE CATALISADORES VO X /Nb 2 O 5 : CARACTERIZAÇÃO DAS PROPRIEDADES ÁCIDAS MEDIANTE A REAÇÃO DE DECOMPOSIÇÃO DO ISOPROPANOL E DTP-NH 3, n.d.

[34] J.B. de Paiva,; W R Monteiro, M.A. Zacharias, J.A.J. Rodrigues,; G G Cortez, INFLUÊNCIA DA ADIÇÃO DE MoO 3 SOBRE CATALISADORES VO X /Nb 2 O 5 : CARACTERIZAÇÃO DAS PROPRIEDADES ÁCIDAS MEDIANTE A REAÇÃO DE DECOMPOSIÇÃO DO ISOPROPANOL E DTP-NH 3, 2006.

[35] W.E. Farneth, E.L. Dupont De, R.J. Gorte, Methods for Characterizing Zeolite Acidity, 1995. https://pubs.acs.org/sharingguidelines.

[36] R.J. Gorte, What do we know about the acidity of solid acids? *, 1999.

[37] E. Lopez Moreno, K. Rajagopal, Desafios Da aciDez na catálise em estaDo sóliDo, 2009.

[38] W. Hu, Y. Liu, R.L. Withers, T.J. Frankcombe, L. Norén, A. Snashall, M. Kitchin, P. Smith, B. Gong, H. Chen, J. Schiemer, F. Brink, J. Wong-Leung, Electron-pinned defect-dipoles for high-performance colossal permittivity materials, Nature Materials. 12 (2013) 821–826. https://doi.org/10.1038/nmat3691.

[39] K. Leiva, N. Martinez, C. Sepulveda, R. García, C.A. Jiménez, D. Laurenti, M. Vrinat, C. Geantet, J.L.G. Fierro, I.T. Ghampson, N. Escalona, Hydrodeoxygenation of 2-methoxyphenol over different Re active phases supported on SiO2 catalysts, Applied Catalysis A: General. 490 (2015) 71–79. https://doi.org/10.1016/j.apcata.2014.10.054.

[40] R. Bassi, M. Villarroel, F.J. Gil-Llambias, P. Baeza, J.L. García-Fierro, N. Martínez, P. Olivera, K. Leiva, N. Escalona, SUPPORT EFFECT ON CONVERSION OF QUINOLINE OVER ReS 2 CATALYST, 2016.

[41] G. Liu, H. Fan, J. Xu, Z. Liu, Y. Zhao, Colossal permittivity and impedance analysis of niobium and aluminum co-doped TiO2 ceramics, RSC Advances. 6 (2016) 48708–48714. https://doi.org/10.1039/c6ra07746c.

[42] J. Okal, W. Tylus, L. Kępiński, XPS study of oxidation of rhenium metal on γ-Al2O 3 support, Journal of Catalysis. 225 (2004) 498–509. https://doi.org/10.1016/j.jcat.2004.05.004.

[43] J. Okal, A study of effect of particle size on the oxidation of rhenium in the Re/γ-Al2O3 catalysts, Applied Catalysis A: General. 287 (2005) 214–220. https://doi.org/10.1016/j.apcata.2005.03.036.

[44] M.T. Greiner, T.C.R. Rocha, B. Johnson, A. Klyushin, A. Knop-Gericke, R. Schlögl, The oxidation of rhenium and identification of rhenium oxides during catalytic partial oxidation

of ethylene: An in-situ xps study, Zeitschrift Fur Physikalische Chemie. 228 (2014) 521–541. https://doi.org/10.1515/zpch-2014-0002.

[45] F.M.T. Mendes, C.A. Perez, R.R. Soares, F.B. Noronha, M. Schmal, Ammonium complex of niobium as a precursor for the preparation of Nb 2 O 5 /Al 2 O 3 catalysts, 2003.

[46] F.P.J.M. Kerkhof, J.A. Moulijn, Quantitative analysis of XPS intensities for supported catalysts, The Journal of Physical Chemistry. 83 (1979) 1612–1619. https://doi.org/10.1021/j100475a011.

[47] P. Biloen, J.N. Helle, H. Verbeek, F.M. Dautzenberg, W.M.H. Sachtler, The Role of Rhenium and Sulfur in Platinum-Based Hydrocarbon-Conversion Catalysts, 1980.

[48] B.L. Mojet, J.T. Miller, D.E. Ramaker, D.C. Koningsberger, A New Model Describing the Metal-Support Interaction in Noble Metal Catalysts, 1999. http://www.idealibrary.comon.

[49] F. Zaera, G.A. Somorjai, THE C~EMISOR~ION OF O, CO, D, AND C&I, OVER EPITAXIALLY GROWN RHENIUM CRYSTALLINE FILMS, 1985.

[50] J.P. da S.Q. Menezes, K.R. Duarte, R.L. Manfro, M.M.V.M. Souza, Effect of niobia addition on cobalt catalysts supported on alumina for glycerol steam reforming, Renewable Energy. 148 (2020) 864–875. https://doi.org/10.1016/j.renene.2019.10.171.

[51] G.F. Leal, S. Lima, I. Graça, H. Carrer, D.H. Barrett, E. Teixeira-Neto, A.A.S. Curvelo, C.B. Rodella, R. Rinaldi, Design of Nickel Supported on Water-Tolerant Nb2O5 Catalysts for the Hydrotreating of Lignin Streams Obtained from Lignin-First Biorefining, IScience. 15 (2019) 467–488. https://doi.org/10.1016/j.isci.2019.05.007.

[52] R. Ladera, E. Finocchio, S. Rojas, J.L.G. Fierro, M. Ojeda, Supported niobium catalysts for methanol dehydration to dimethyl ether: FTIR studies of acid properties, in: Catalysis Today, 2012: pp. 136–143. https://doi.org/10.1016/j.cattod.2012.01.025.

[53] S. den van Hark, M. Härröd, Fixed-bed hydrogenation at supercritical conditions to form fatty alcohols: The dramatic effects caused by phase transitions in the reactor, in: Industrial and Engineering Chemistry Research, American Chemical Society, 2001: pp. 5052–5057. https://doi.org/10.1021/ie000951l.

[54] T. Miyake, T. Makino, S. ichi Taniguchi, H. Watanuki, T. Niki, S. Shimizu, Y. Kojima, M. Sano, Alcohol synthesis by hydrogenation of fatty acid methyl esters on supported Ru-Sn and Rh-Sn catalysts, Applied Catalysis A: General. 364 (2009) 108–112. https://doi.org/10.1016/j.apcata.2009.05.036.

[55] J. Datka, A.M. Turek, J.M. Jehng, I.E. Wachs, Acidic Properties of Supported Niobium Oxide Catalysts: An Infrared Spectroscopy Investigation, 1992.

[56] F. Passos, Effect of preparation method on the properties of Nb2O5 promoted platinum catalysts, Catalysis Today. 43 (1998) 3–9. https://doi.org/10.1016/S0920-5861 (98)00131-X.

[57] J.-M. Jehng, I.E. Wachs, Niobium Oxalate, in: 1990: pp. 232–242. https://doi.org/10.1021/bk-1990-0437.ch021.

[58] L.L. Murrell, D.C. Grenoble, C.J. Kim, N.C. Dispenziere, Supported Transition Metal Oxides as Acid Cracking Catalysts: Periodic Trends and Their Relationship to Activity and Selectivity, 1987.

[59] D.S. Thakur, B.D. Roberts, G.T. White, R.D. Rieke, Fatty methyl ester hydrogenation to fatty alcohol: Reaction inhibition by glycerine and monoglyceride, J Am Oil Chem Soc. 76 (1999) 995–1000. https://doi.org/10.1007/s11746-999-0118-z.